Light Scattering and Heterogeneities in Low-Loss Poly(methyl methacrylate) Glasses

Yasuhiro Koike,* Norihisa Tanio, and Yasuji Ohtsuka

Faculty of Science and Technology, Keio University, 3-14-1, Hiyoshi, Kohoku-ku, Yokohama, 223, Japan. *Received May 27, 1988; Revised Manuscript Received September 6, 1988*

ABSTRACT: A poly(methyl methacrylate) (PMMA) glass was prepared for the first time, in which the light-scattering loss was much smaller than any reported data and no large size of heterogeneities existed. The total scattering loss was 13 dB/km which represents an intrinsic limiting loss of the PMMA glasses attainable in the atmosphere. The isotropic scattering loss widely varied between ca. 9 and 400 dB/km according to the conditions of polymerization or heat treatment, while the anisotropic scattering loss was almost unchanged in the range 4–6 dB/km. The origins of the large heterogeneities with the dimension of ca. 1000 Å, which have been invariably observed in PMMA glasses reported so far, were investigated by the angular dependence of the light scattering. The large excess scattering is caused mainly by the isotropic strain inhomogeneities caused during polymerization and not by a small amount of remaining monomers or additives, the molecular weight of polymers, the stereoregularity due to the specific tacticity of PMMA, or cross-linking as a result of the gel effect.

Introduction

Many models have been proposed to depict the local structure of apparently amorphous polymer glasses. These models are mainly divided into two categories. One is the "coil model",[1,2] where the amorphous phase is homogeneous and random in structure and the molecular conformation in polymer glasses is considered to be the same as in θ-solvent. The other is the so-called "bundle model",[3-5] where the amorphous phase is not homogeneous and nodular structures such as bundles of parallel molecular chains or folded chains exist.

A nodular structure supporting the bundle model was observed in several polymer melts by electron diffraction.[6] On the contrary, the coil model has been supported by radiation scattering techniques such as neutron,[7,8] X-ray,[9-11] and Rayleigh–Brillouin[12] scattering. For instance, small-angle neutron scattering for a few polymers such as poly(methyl methacrylate) (PMMA)[7] or polystyrene (PSt)[8] revealed that the radii of gyration in the bulk were well consistent with those in dilute solution. From small-angle X-ray scattering, the conformation of the polymer chain in the bulk was found to be a Guassian coil as suggested by Flory, and no orders indicating some anisotropic structures described by various bundle models were observed.

On the other hand, light-scattering measurements have been widely used[13-20] to describe the local structure of bulk polymers in the range between hundreds to thousands of angstroms. Even in the highly purified PMMA bulk in which no anisotropic orders observed by neutron or X-ray scatterings exist, large size heterogeneities with the dimension of about 1000 Å have been invariably observed by the angular dependence of polarized light scattering (V_V).[18-21] Fischer and co-workers suggested that these heterogeneities are not related to the chain configuration,[2] since no coinciding anisotropy fluctuations were observed. These heterogeneities cause large excess V_V scattering and angular dependence in its intensity.

As origins of these heterogeneities, extrinsic impurities such as residual monomers or additives, the formation of cross-linking as the result of "gel effect" during polymerization, stereoregularity according to specific tacticities, the effect of high molecular weight, and internal frozen strain have been suggested so far. However, in a pure PSt bulk, no such heterogeneity has been observed.[22] In spite of a significant number of works concerned with this problem, the origin of this large heterogeneous structure is still obscure.

The temperature dependence of the V_V scattering around a glass transition temperature has been examined[18] to clarify whether the thermally induced density fluctuation would be inherent in the polymer bulk as well as in liquids. However, the intensities of the excess V_V scattering observed in these bulk polymers were much larger than that predicted in this fluctuation theory, and the large heterogeneities exist inside the examined polymer bulk. Therefore, unless a sample with no large heterogeneity is used, no persuasive conclusion about this thermally induced density fluctuation can be derived.

In this paper, the bulk PMMA, which has light-scattering loss much smaller than any reported data and no large heterogeneous structure, was prepared for the first time.[23] Thus it became possible to independently investigate each hypothesized origin of the excess light scattering having the angular dependence, as mentioned above. The inherent effects of the small amount of impurities or remaining monomers, specific tacticities, and the molecular weight of the polymer on the V_V scattering were quantitatively clarified. The ambiguous effects of these on the excess light scattering became, we believe, clear in this paper.

Low-loss PMMA bulk is useful as a material for polymer optical fibers[24] or other optical waveguides.[25] In these uses, a very slight amount of heterogeneity inside the PMMA glass causes the large effect on the light-scattering loss. The transmission loss through the polymer optical fiber has been governed by the scattering loss due to the heterogeneities. It was theoretically and experimentally confirmed that by improving the local structure the scattering loss in the purified PMMA was decreased from hundreds of dB/km to 13 dB/km which is presumably an inherent limiting loss for the PMMA bulk in the atmosphere.

Experimental Section

Preparation of PMMA Bulk. In order to eliminate the effect of unknown impurities on the light scattering, the PMMA sample was prepared as follows: First, inhibitors in the MMA monomer were removed by rinsing with 0.5 N NaOH aqueous solution, followed by washing out the slight amount of NaOH with pure water. The monomer was dried over anhydrous sodium sulfate, filtered through a 0.2-μm membrane filter, and distilled under reduced pressure (bp 46–47 °C (100 mmHg) into a purified ampule A.

Further, a rigorous purification was carried out as follows: The ampule A with the distilled monomer was connected with two ampules B and C, which were carefully cleaned. Here, di-*tert*-butyl peroxide (DBPO) as an initiator and *n*-butylmercaptan (nBM) as a chain-transfer agent were placed in ampule B, and

0024-9297/89/2222-1367$01.50/0

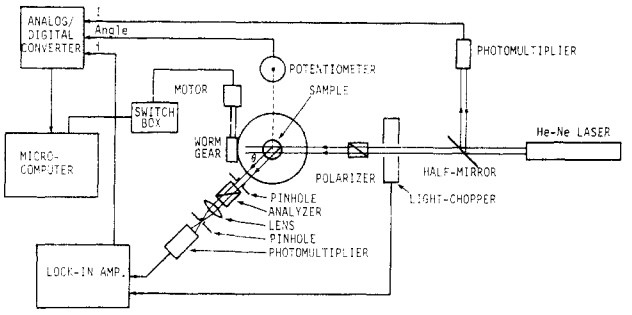

Figure 1. Diagram of light-scattering measurement system.

ampule C was empty. Ampules A and B were frozen with liquid nitrogen, evacuated, and filled with nitrogen. Then MMA, DBPO, and nBM were outgassed by several freeze–thaw cycles and slowly distilled into ampule C under vacuum by cooling ampule C with liquid nitrogen. When glitterings due to impurities in the monomer mixture were noted by a He–Ne laser beam; the monomer mixture in ampule C was tipped back into ampule A and redistilled under vacuum into ampule C. This process was repeated until no glittering was detected in the distilled monomer mixture. Finally ampule C was sealed under vacuum and was immersed in silicone oil for polymerization. After the polymerization under various conditions, the resulting cylindrical PMMA sample with a 20-mm diameter was taken out of ampule C for measurement of the light scattering.

Light Scattering Measurement. Figure 1 shows our measurement system of the light-scattering intensity. The light source was a 7-mW polarized He–Ne laser (wavelength, 633 nm) which was set up to obtain vertical polarization. The laser beam was divided into two by a half-mirror. One was directly monitored by a photomultiplier tube (PMT) to compensate for the fluctuation of the laser intensity. The other beam passed through a light chopper and a polarizer (Glan Tompson prism) and then entered the sample from the side.

The sample was placed in the center of the cylindrical glass cell. The gap between the sample and the inner wall of the glass cell was filled with immersion oil whose index of refraction was 1.5. This glass cell was perpendicularly located on the center of the goniometer. The scattered light from the sample passed through pinhole A (1-mm diameter)–analyzer (Glan Tompson prism)–converging lens–pinhole B (0.1-mm diameter) and was detected by a PMT (Hamamatsu Photonics Co., Model R928). Since pinhole B is located just on the focal point of the converging lens, only nearly parallel rays scattered from the center of the sample were detected. The validity of this conclusion was confirmed by the fact that there was no difference in measurement intensities observed by changing the length (5–30 cm) between the sample and pinhole A. Considering the parallel incident beam and the parallel scattered beam, the scattering volume viewed from the PMT is inversely proportional to $\sin\theta$. Here θ is the scattering angle defined between the incident and scattering beams. Therefore, the observed intensity was multiplied by $\sin\theta$ to obtain normalized V_V (polarized) and H_V (depolarized) scatterings.

The setting of the scattering angle and the measurement of the scattering intensity were all operated by a microcomputer. At a fixed scattering angle, the scattering intensities were measured 200 times, and this average was employed for data analysis. With a light chopper–lock-in amplifier system, the S/N ratio of the signal even for weak scattering light was sufficiently improved. The measurement error of the scattering intensity (V_V or H_V) in the order of 10^{-8} cm^{-1} was less than 2%.

In this paper, V_V and H_V intensities were measured. To estimate the absolute intensities of these, pure benzene which was purified in the same manner as the monomer mixture mentioned above was used as a standard for calibration. The observed depolarization factor ρ was 0.42 and was close to the published value of 0.43 (633-nm wavelength).[26] V_V and H_V for pure benzene had no angular dependence in the range of θ = 30–120°, which indicated that all optical parts were properly set up and no stray light was included in the detected intensity.

Determination of the Tacticity of PMMA. After the PMMA sample was dissolved in a small amount of acetone, a large excess of methanol was added to the solution to precipitate the polymer. The polymer dried under reduced pressure was used as a sample to determine the tacticity by ^{1}H NMR (Varian Model EM-390) spectroscopy. The NMR spectra were taken with $CDCl_3$ polymer solution (10 wt %) at 25 °C. Three peaks for the α-methyl group of PMMA at 0.82, 1.03, and 1.20 ppm correspond to syndio-, hetero-, and isotactic configurations, respectively. Therefore, the triad tacticity was determined by measuring the peak area ratio of these chemical shifts.

Other Measurements. The glass transition temperatures (T_g) of polymers were measured by differential scanning calorimeter (DSC) (Perkin-Elmer DSC-1B), at a heating rate of 32 °C/min. The birefringence of sample B was measured by a precise stress–strain measurement instrument (Toshiba Glass Co., Model SVP-30). The molecular weight and its distribution were measured by gel permeation chromatography (GPC) (column; Showa denko Co., Shodex AC-80M, RI; Showa denko Co., Shodex RI SE-11) with chloroform as a carrier.

The weight percentage of the remaining monomer in the PMMA bulk was measured as follows: The polymer sample was dissolved in a small amount of acetone, followed by adding methanol to precipitate the polymer. A slight amount of monomer in the supernatant solution was measured by gas chromatography. The weight percentage of the monomer was determined from the corresponding peak area of the chart.

Theory

When natural light with an intensity I_0 passes through a distance y and its intensity is decreased to I by the scattering loss, the turbidity τ is defined by eq 1. Since

$$I/I_0 = \exp(-\tau y) \tag{1}$$

the turbidity τ corresponds to the summation of all light scattered to all directions, τ is given by eq 2. Here symbols

$$\tau = \pi \int_0^{\pi} (V_V + V_H + H_V + H_H) \sin\theta \, d\theta \tag{2}$$

V and H denote vertical and horizontal polarizations, respectively. The symbol A of the scattering component A_B represents the direction of an analyzer and the subscript B represents the direction of the polarizing phase of an incident light. θ is the scattering angle from the direction of the incident ray.

In structureless liquid or randomly oriented polymer bulk, these intensities are given by the following equations:[27]

$$V_H = H_V \tag{3}$$

$$H_H = V_V \cos^2\theta + H_V \sin^2\theta \tag{4}$$

As shown later, almost all samples exhibited angular dependence in the V_V intensity due to large heterogeneities inside the bulk. Then, we separated V_V into two terms as written in eq 5, where V_{V1} denotes a background intensity

$$V_V = V_{V1} + V_{V2} \tag{5}$$

which is independent of the scattering angle and V_{V2} is the excess scattering with angular dependence due to large heterogeneities. The isotropic part V_{V1}^{iso} of the V_{V1} is given by eq 6. When there is no angular dependence in H_V, the

$$V_{V1}^{iso} = V_{V1} - \tfrac{4}{3}H_V \tag{6}$$

angular dependence of V_V is attributed to the isotropic scattering V_{V2}^{iso}. Therefore

$$V_{V2} = V_{V2}^{iso} \tag{7}$$

By substitution of eq 3–7 into eq 2

$$\tau = \pi \int_0^{\pi} \left\{ (1 + \cos^2\theta)(V_{V1}^{iso} + V_{V2}^{iso}) + \frac{(13 + \cos^2\theta)}{3} H_V \right\} \sin\theta \, d\theta \tag{8}$$

For the V_{V2}^{iso}, Debye et al. derived eq 9,[28] where $\langle\eta^2\rangle$ denotes the mean-square average of the fluctuation of all

$$V_{V2}^{iso} = \frac{4\langle\eta^2\rangle\pi^3}{\lambda_0^4}\int_0^\infty \frac{\sin(\nu sr)}{\nu sr} r^2\gamma(r)\,dr \qquad (9)$$

dielectric constants, $\nu = 2\pi/\lambda$, and $s = 2\sin(\theta/2)$. λ and λ_0 are wavelengths of light in a specimen and under vacuum, respectively. $\gamma(r)$ refers to the correlation function defined by $\eta_i\eta_j/\langle\eta^2\rangle$ where η_i and η_j are the fluctuations of dielectric constants at i and j positions. Assuming that the correlation function is expressed by eq 10 as suggested by Debye et al.,[28] eq 9 is simply integrated to give eq 11.

$$\gamma(r) = \exp(-r/a) \qquad (10)$$

$$V_{V2}^{iso} = \frac{8\pi^3\langle\eta^2\rangle a^3}{\lambda_0^4(1+\nu^2s^2a^2)^2} \qquad \nu = 2\pi n/\lambda_0 \qquad s = 2\sin(\theta/2) \qquad (11)$$

Here a is called the correlation length and is a measure of the size of the heterogeneous structure inside the bulk.

The turbidity τ is divided into three terms. Namely

$$\tau = \tau_1^{iso} + \tau_2^{iso} + \tau^{aniso} \qquad (12)$$

where τ_1^{iso} is the turbidity coming from the V_{V1}^{iso} scattering, τ_2^{iso} is from V_{V2}^{iso}, and τ^{aniso} is from the anisotropic scattering, H_V. From eq 8, these terms are given as follows:

$$\tau_1^{iso} = \pi\int_0^\pi (1+\cos^2\theta)V_{V1}^{iso}\sin\theta\,d\theta = {}^8/_3\pi V_{V1}^{iso} \qquad (13)$$

$$\tau_2^{iso} = \frac{32a^3\langle\eta^2\rangle\pi^4}{\lambda_0^4}\left\{\frac{(b+2)^2}{b^2(b+1)} - \frac{2(b+2)}{b^3}\ln(b+1)\right\} \qquad b = 4k^2a^2 \qquad (14)$$

$$\tau^{aniso} = {}^{80}/_9\pi H_V \qquad (15)$$

The light-scattering loss α (dB/km) is related to the turbidity τ (cm^{-1}) by eq 16. The light-scattering losses

$$\alpha\ (\mathrm{dB/km}) = 4.342\times10^5\tau\ (\mathrm{cm^{-1}}) \qquad (16)$$

corresponding to each turbidity of eq 12–15 are defined as α_t, α_1^{iso}, α_2^{iso}, and α^{aniso}, respectively. That is

$$\alpha_t = \alpha_1^{iso} + \alpha_2^{iso} + \alpha^{aniso} \qquad (17)$$

Again, these scattering losses in our treatment are based on the following two assumptions: (1) The H_V is independent of the scattering angle and no large anisotropic order exists. (2) The V_{V2}^{iso} given by eq 11 is superimposed on the constant background V_{V1}.

Results and Discussion

Before obtaining quantitative scattering data through the above analysis, we have to confirm the validity of the above two assumptions. For assumption 1, all PMMA samples prepared in our laboratory had no angular dependence in the H_V intensities which were in the range 3–6 $\times 10^{-7}$ cm^{-1}, while many samples strongly exhibited the forward excess V_V scattering. Therefore, it is clear that the angular dependence was due to the isotropic heterogeneity and not due to the anisotropic order. Thus, assumption 1 seems reasonable in our experiment.

For assumption 2, it is difficult to experimentally discriminate the V_{V2}^{iso} component from the observed V_V. Thus the following procedure was carried out. By the rearrangement of eq 11, $V_{V2}^{-1/2}$ versus s^2 (Debye plot) gives a straight line, and the correlation length a can be determined by $a = (\lambda/2\pi)(\mathrm{slope/intercept})^{1/2}$. Therefore by changing the V_{V2}^{iso} value between 0 and the observed V_V little by little, the V_{V2}^{iso} where the Debye plot became closest to a straight line was obtained by a least-square technique in a computer and was employed in data analysis.

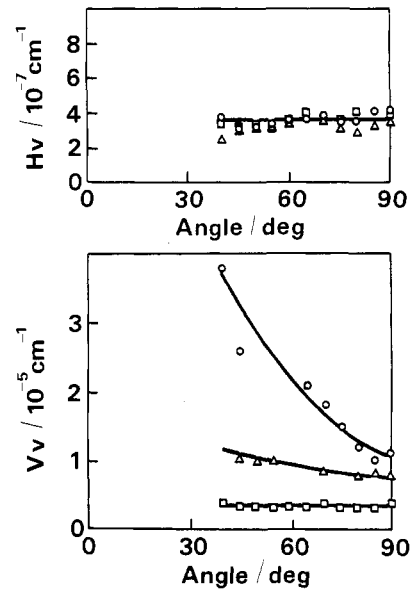

Figure 2. V_v and H_v scattering by PMMA glasses polymerized at 70 °C (○), 100 °C (△), and 130 °C (□) for 96 h.

Table I
Scattering Parameters of PMMA Glasses Polymerized at 70, 100, and 130 °C for 96 h

polymeriztn temp, °C	a, Å	$\langle\eta^2\rangle$, 10^{-8}	α_1^{iso}, dB/km	α_2^{iso}, dB/km	α^{aniso}, dB/km	α_t, dB/km
70	676	1.05	16.8	40.8	4.4	62.0
100	466	0.53	17.7	10.9	4.0	32.6
130		0	9.7	0	4.7	14.4

Figure 2 shows the effect of the polymerization temperature on the V_V and H_V scattering intensities. PMMA samples were polymerized at 70, 100, and 130 °C, respectively, for 96 h. The weight percentages of DBPO and nBM were both 0.2 wt %. (Unless otherwise noted, the concentrations of DBPO and nBM were both 0.2 wt % in this paper.) With an increase in the polymerization temperature, the V_V intensity decreased, and no angular dependence was observed at 130 °C, while the H_V values for these were almost the same in the range 3–4 $\times 10^{-7}$ cm^{-1}. Scattering data and structural parameters of these PMMA samples are summarized in Table I. With the increase in polymerization temperature, the total scattering loss α_t remarkably decreased from 62 to 14.4 dB/km, where α_2^{iso} from the isotropic V_{V2}^{iso} due to large heterogeneities decreased from 41 dB/km to 0, although the anisotropic scattering loss α^{aniso} was almost invariant around 4–5 dB/km. It is clear from Table I that the excess V_V scattering expressing the angular dependence is not inherent in the PMMA bulk.

The intensity of the isotropic V_V^{iso} scattering from thermally induced density fluctuations in a structureless liquid is given by[29]

$$V_V^{iso} = \frac{\pi^2}{9\lambda_0^4}(n^2-1)^2(n^2+2)^2kT\beta \qquad (18)$$

where k is the Boltzmann's constant, T the absolute temperature, and β the isothermal compressibility. With published values[17] $\beta = 3.55\times10^{-11}$ cm^2/dyn around T_g for the PMMA bulk, assuming a frozen condition, the V_V^{iso}

Table II
Properties of PMMA Glasses Polymerized at 70, 100, and 130 °C for 96 h

polymeriztn temp, °C	M_w, 10^4	M_w/M_n	T_g, °C	remaining monomer, wt %	P_h/P_s
70	8.5	4.1	80	5.5	0.69
100	6.8	2.5	98	1.4	0.86
130	6.5	2.8	111	1.2	0.93

calculated from eq 18 at room temperature for 633-nm wavelength is 2.61×10^{-6} cm^{-1}. By eq 13 and 16, the light-scattering loss from this V_V^{iso} value is estimated to be 9.5 dB/km which is very close to 9.7 dB/km of the α_1^{iso} for the sample polymerized at 130 °C in Table I. Therefore, if eq 18 using β at T_g is applicable to the polymer bulk, the value of 9.7 dB/km attained in Table I would be the limit of the isotropic scattering loss for the PMMA in the atmosphere.

It is clear from Table I that the large decrease in the excess scattering is mainly attributed to the disappearance of the isotropic heterogeneous structure in which the correlation length is about 700 Å and the $\langle\eta^2\rangle$ is about 10^{-8}. If it is assumed that this heterogeneous structure consists of two phases whose volume fractions are ϕ_1 and ϕ_2 and whose refractive indices are n_1 and n_2, respectively, $\langle\eta^2\rangle$ is given by

$$\langle\eta^2\rangle = \phi_1\phi_2(n_1^2 - n_2^2)^2 \quad (19)$$

In the sample polymerized at 70 °C in Table I, since $\langle\eta^2\rangle = 1.05 \times 10^{-8}$, the difference of refractive indices between the two phases $\Delta n = n_1 - n_2$ are $\Delta n = 3.4 \times 10^{-4}$ for $\phi_1 = 0.01$, $\Delta n = 1.1 \times 10^{-4}$ for $\phi_1 = 0.1$, and $\Delta n = 6.7 \times 10^{-5}$ for $\phi_1 = 0.5$.

As far as the origin of this heterogeneous structure leading to the excess scattering is concerned, many speculations have been proposed so far, e.g., low molecular impurities such as residual monomer or additives, the formation of cross-links or bulky side chains as the result of the "gel effect" during polymerization, stereoregularity according to the configuration of specific tacticities, the effect of high molecular weight, and the formation of microvoids or internal frozen strain. However, in spite of extensive work directed to this excess scattering, these speculations remain ambiguous hypotheses, because the relation between the scattering and each effect mentioned above has not been quantitatively and independently discussed.

In Table II are shown the chemical and physical properties of samples in Table I. With an increase in the polymerization temperature, the weight-average molecular weight M_w decreased from 8.5×10^4 to 6.5×10^4, the remaining monomer decreased from 5.5 wt % to 1.2 wt %, and the T_g increased with a decrease of remaining monomer. As for the tacticity in the triad expression, the ratio of the heterotactic placement to syndiotactic, P_h/P_s, increased from 0.69 to 0.93, approaching the random configuration. Therefore, several effects which might decrease the excess scattering varied simultaneously, which made the quantitative analysis difficult.

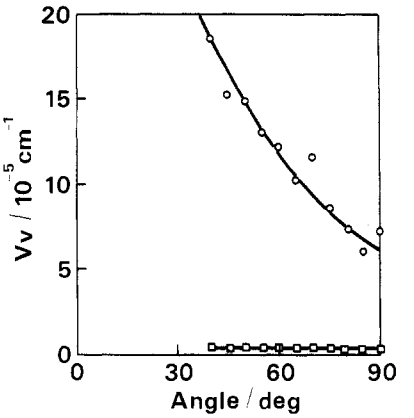

Figure 3. V_v scattering by PMMA glasses polymerized at 70 °C for 216 h (○) and 130 °C for 96 h–180 °C for 48 h (□).

In this paper, the effect of each property on the excess scattering was observed independently by the following procedure.

Effect of Small Molecules. Figure 3 shows the V_V scattering of two PMMA samples. One was polymerized at 70 °C for 216 h. The other was polymerized at 130 °C for 96 h, followed by heat-treatment at 180 °C for 48 h. The scattering data are listed in Table III with the weight-average molecular weight and the weight fraction of the remaining monomer. While the sample polymerized at 70 °C had very large scattering loss $\alpha_t = 360$ dB/km and a heterogeneous structure with $a = 558$ Å, the other sample polymerized at 130 °C had much smaller scattering loss $\alpha_t = 13.6$ dB/km with no angular dependence in the V_V intensity. It is quite noteworthy that the monomer weight fractions detected by gas chromatography for both samples are almost the same, namely 4.7 and 4.4 wt %, respectively. With respect to the latter sample, the remaining monomer fraction after the polymerization at 130 °C for 96 h was 1.2 wt % as shown in Table II. However, during the subsequent heat treatment, the remaining monomer increased up to 4.4 wt % by depolymerization because the polymerization temperature was close to the ceiling temperature ca. 210 °C of PMMA. The difference of the monomer concentration between 4.7 and 4.4 wt % in Table III is too small to explain the dramatic decrease of α_2^{iso} from 317 dB/km to 0.

Furthermore, in order to confirm the effect of the remaining monomer, the MMA monomer mixture which included a small amount of methyl propionate (MP) as the model compound of MMA monomer was polymerized at 130 °C for 24 h, 150 °C for 24 h, and 180 °C for 24 h. Since the MP is not polymerizable, the added MP remains unpolymerized in the completely polymerized PMMA. The refractive indices of MP and MMA monomer are 1.38 and 1.42, respectively, and the refractive index of the PMMA is 1.49. The V_V scattering of the sample with MP = 3 wt % is shown in Figure 4 along with the pure PMMA which was polymerized in the same manner. It is very interesting that the two samples with sufficient heat treatment had almost the same V_V intensities with no angular dependence, and the α_1^{iso} values for both samples were about 10

Table III
Properties of PMMA Glasses Polymerized at (S1) 70 °C for 216 h and (S2) 130 °C for 96 h Followed by 180 °C for 48 h

sample	a, Å	$\langle\eta^2\rangle$, 10^{-8}	α_1^{iso}, dB/km	α_2^{iso}, dB/km	α^{aniso}, dB/km	α_t, dB/km	M_w, 10^4	remaining monomer, wt %
S1	558	11.2	37.2	316.8	6.3	360.3	10.7	4.7
S2		0	7.2	0	6.4	13.6	6.3	4.4

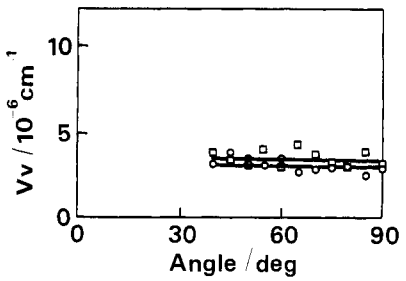

Figure 4. V_v scattering by PMMA glasses polymerized at 130 °C for 96 h–150 °C for 24 h–180 °C for 24 h. Methyl propionate 0 wt % (○) and 3 wt % (□).

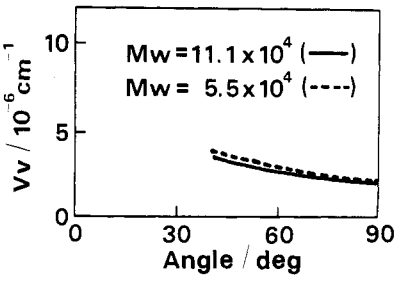

Figure 5. V_v scattering by PMMA glasses polymerized at 70 °C for 88 h–150 °C for 24 h (—) and 130 °C for 96 h–150 °C for 24 h (- - -).

dB/km, which is about the limit value estimated from the thermally induced fluctuation theory, eq 18.

When such small molecules are not localized, they do not form a large heterogeneous region, and then the V_{V2}^{iso} in eq 11 having angular dependence becomes negligibly small. As for the V_V^{iso} in eq 18 caused by thermally induced fluctuations, a slight amount of small molecules decreases the T_g, probably leading to a slight increase in the isothermal compressibility β, which is proportional to the V_V^{iso}. Although we have not measured β for these samples, the above fact that the addition of 3 wt % MP scarcely increased the V_V intensity would imply that β is not largely changed by MP.

We conclude that if small molecules such as remaining monomers are not localized in the polymer bulk, small molecules in the concentration range of several weight percentages do not inherently affect the excess V_V scattering.

Effect of Molecular Weight of Polymer. As shown in Table II, with an increase in the polymerization temperature from 70 to 130 °C, the molecular weight M_w decreased from 8.5×10^4 to 6.5×10^4, and the total light-scattering loss α_t decreased from 62.0 to 14.4 dB/km as shown in Table I. In Table III, with a decrease in the M_w from 1.07×10^5 to 6.3×10^4, the α_t remarkably decreased from 360 to 13.6 dB/km. Such similar results have been already reported, and a correlation between the molecular weight and the excess light scattering has been suggested.

The aggregation or entanglement behavior of polymer chains would be dependent on the molecular weight. Therefore, the speculation that the excess V_v scattering would increase with increasing the molecular weight is reasonable. However, this trend was, in this work, the case only for the sample polymerized below T_g with no special heat treatment above T_g. It was quite interesting to find that if the above samples with different molecular weights were sufficiently heat treated above T_g, all samples had almost the same V_V scattering intensities. The effect of the heat treatment is discussed later. For instance, Figure 5 shows the V_V scattering of two samples whose molecular weights M_w are 5.5×10^4 (dotted line) and 1.1×10^5 (solid line). These two V_V scattering intensities were almost the same. The sample with $M_w = 5.5 \times 10^4$ was polymerized at 130 °C for 96 h and heat treated at 150 °C for 24 h, while the sample with $M_w = 1.1 \times 10^5$ was polymerized at 70 °C for 88 h and heat treated at 150 °C for 24 h. The remaining monomer for the former was about 1 wt % and for the latter about 2 wt %.

It is clear that the excess V_V scattering would be, in essence, independent of the molecular weight of the polymer at least in the range of any M_w mentioned above.

Effect of Stereoregularity of the PMMA Polymer. As explained in Tables I and II, with an increase in the tacticity ratio P_h/P_s (heterotactic to syndiotactic) from 0.69 to 0.93 approaching a random configuration, the scattering loss α_2^{iso} due to large heterogeneities with a = 680 Å decreased from 41 dB/km to 0. With respect to the tacticity in PMMA, evidence of stereoassociation complexes[30] or self-association[31] has been reported. Since polystyrene, which is an atactic polymer, had no excess angular-dependent V_V scattering,[22] it is important to investigate the effect of the specific tacticity of the PMMA on the excess scattering.

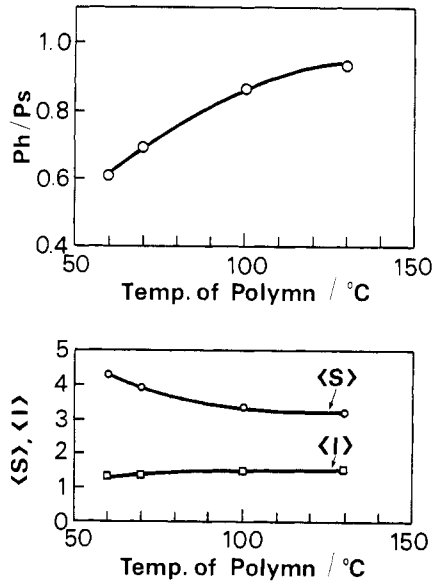

Figure 6. Effect of polymerization temperature on tacticities of PMMA glasses.

To discuss the possibility of forming stereoregularity along polymer chains in the free radical polymerization, the average lengths of successive syndiotactic, heterotactic, and isotactic units, designated as ⟨s⟩, ⟨h⟩, and ⟨i⟩, respectively, were calculated. When the probability of obtaining meso or racemic diad is independent of the configuration of the growing polymer chain, the average successive lengths of each triad sequence, ⟨s⟩, ⟨i⟩, and ⟨h⟩, are written by eq 20.[32] The validity of this assumption in the radical polymerization of the MMA has been well-known.[33]

$$\langle s \rangle = 1 + \frac{2P_s}{P_h} \qquad \langle i \rangle = 1 + \frac{P_h}{2P_s} \qquad \langle h \rangle = 2 \tag{20}$$

PMMA samples with different tacticities were prepared by changing the polymerization temperature from 60 to 130 °C. In Figure 6 are shown the average syndio- and isotactic successive lengths, ⟨s⟩ and ⟨i⟩, obtained by eq 20, and P_h/P_s for these polymerized samples. With an increase in the polymerization temperature from 60 to 130 °C, P_h/P_s increased from 0.61 to 0.93, and T_g decreased from 114 to 89 °C because the T_g's of iso- and syndiotactic PMMA glasses are 45 and 115 °C, respectively. However, it is noticed that in the range of the polymerization tem-

Table IV
Properties of PMMA Glasses Polymerized at (A) 70 °C for 96 h, (B) 70 °C for 216 h, and (C) 70 °C for 216 h-(Gradually Increasing Temperature)-180 °C for 24 h

sample	a, Å	$\langle\eta^2\rangle$, 10^{-8}	α_1^{iso}, dB/km	α_2^{iso}, dB/km	α^{aniso}, dB/km	α_t, dB/km	T_g, °C	remaining monomer, wt %
A	676	1.05	16.8	40.8	4.4	62.0	80	5.5
B	558	11.20	37.2	316.8	6.3	360.3	86	4.7
C		0	8.9	0	4.0	12.9	102	1.7

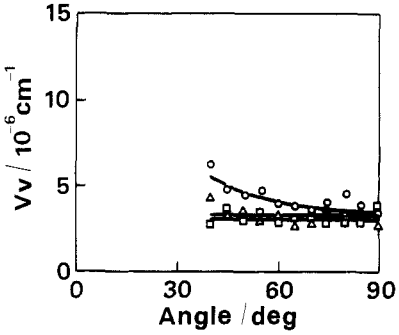

Figure 7. V_v scattering by PMMA glasses polymerized at 60 °C (○), 70 °C (△), and 130 °C (□) for 96 h. All samples were heat treated at 180 °C for 24 h.

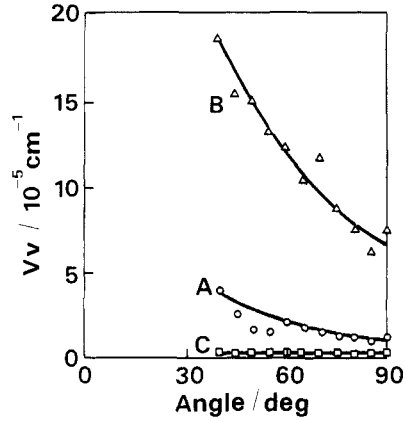

Figure 8. V_v scattering by PMMA glasses polymerized as follows: (A) 70 °C for 96 h; (B) 70 °C for 216 h; (C) 70 °C for 216 h–(gradually increasing temperature)–180 °C for 24 h.

perature between 70 and 130 °C, ⟨s⟩ and ⟨i⟩ are slightly changed but always less than four units. Even if the association of polymer chains is assumed, four units seem to be too small to explain the presence of large heterogeneities such as a = 700 Å. And if this is the case, the H_V intensity should express the angular dependence due to the anisotropic order. However, for all samples examined above, the H_V was around 3–6 × 10^{-7} cm^{-1} without any angular dependence.

Figure 7 shows the V_V scattering of the sample polymerized at corresponding temperatures for 96 h. All samples were heat treated at 180 °C for 24 h, after gradually increasing the temperature up to 180 °C. By this sufficient heat treatment, the V_V intensity for the sample polymerized below the T_g of PMMA was remarkably decreased, as is evident in comparison with the V_V in Figure 2. It is very interesting that the V_V intensities of the samples polymerized at 70 and 130 °C were almost the same, ca. 3 × 10^{-6} cm^{-1} without any angular dependence. Since the tacticity is not changed by the heat treatment, the difference of the V_V intensities in Figure 2 cannot be explained by the difference in the tacticity.

These results lead to the conclusion that the stereoregularity in the range shown in Figure 6 does not inherently cause the excess V_V scattering.

Effect of Heat Treatment. The heat treatment seems to be most important factor which affects the excess V_V scattering. Figure 8 shows the effect of the heat treatment below and above T_g on the V_V intensity. The properties of these samples are listed in Table IV. Samples A and B were polymerized at 70 °C for 96 and 216 h, respectively. Sample C was obtained by subsequently heat treating sample B at 180 °C. It is quite interesting to point out that when sample A was continuously heated at 70 °C (below T_g), the V_V intensity gradually increased, decreasing the remaining monomer by 0.7 wt % as shown in Table IV. However, when this sample B was heat treated at 180 °C (above T_g), the V_V intensity remarkably decreased nearly to the theoretical limitation predicted by eq 18.

Thus we can say that the T_g is the critical temperature for determining the excess V_V, and once the sample is polymerized or heat treated above the T_g, the excess V_V intensity almost disappears. Such an effect was also observed in Brillouin scattering[34] in PMMA glasses. Furthermore, the temperature dependence of the V_V intensity around T_g was examined. It was clearly pointed out that, in sample C with no excess scattering in Table IV, V_{V1}^{iso} versus temperature was quite consistent with V_V^{iso} of eq 18. On the other hand, in sample B with large heterogeneities, an abrupt decrease in V_{V1}^{iso} around T_g was observed, which is qualitatively consistent with that reported by Fischer et al.[18] Details concerning the temperature dependence of the two types of PMMA glasses will be reported soon.[35]

In the case of PMMA, the volume contraction in the polymerization process is about 20%. It is reasonable to consider that below T_g the conversion from monomer to polymer would cause some strain inhomogeneities composed of dense and sparse domains, while above T_g, these fluctuations would be relaxed to be homogeneous. These inhomogeneities seem to be almost isotropic, because the H_V intensities for these samples were almost unchanged before and after the heat treatment above T_g.

Photoelasticity coefficients for the following two samples were measured to investigate the above effect. One was polymerized at 70 °C for 240 h (α_t = 734 dB/km, residual monomer = 4.0 wt %, density = 1.187). The other was polymerized at 130 °C for 96 h and at 180 °C for 48 h (α_t = 13.6 dB/km, residual monomer = 4.4 wt %, density = 1.188). The photoelasticity coefficient for the former was 4.0 × 10^{-7} cm^2 kg^{-1} and for the latter 6.0 × 10^{-7} cm^2 kg^{-1}. It is interesting that although the amount of remaining monomer in the former was slightly less than that in the latter, the photoelasticity coefficient and the density in the former were smaller. One would anticipate that in the former sample the sparse domain of inhomogeneous structure, which is caused by the volume contraction during polymerization, or resulting monomer segregation would act as a buffer to depress the photoelasticity coefficient.

The strain inhomogeneity caused at high monomer conversion seems to be a dominant factor for the excess scattering.

Effect of Birefringence by Stress–Strain. Figure 9a shows a picture of the cross section of sample B in

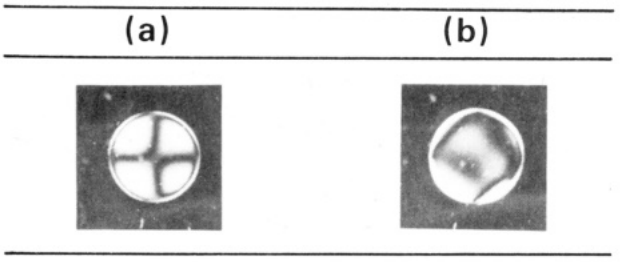

Figure 9. Observation of PMMA samples by the orthogonal Nicol method: (a) polymerized at 70 °C for 216 h; (b) polymerized at 70 °C for 216 h and enough heat treatment at 150 °C.

Figure 8 (20-mm diameter and 10-mm length) polymerized at 70 °C for 216 h, observed by the orthogonal Nicol system in which the principal axes of two Nicol prisms were vertical and horizontal, respectively. When the birefringence exists in the radial direction, a cross-shaped pattern is observed. It is apparent that sample B has radial birefringence. On the other hand, sample B was heat treated at 150 °C in a glass tube whose diameter was slightly larger than that of the sample. As shown in Figure 9b, the above cross-shaped birefringence disappeared and the whole cross section became dark, which implies that this sample was homogeneous with no birefringence. The birefringence expressed by the difference of refractive index was ca. 5 $\times 10^{-6}$ in the cross section of the sample.

It is noteworthy that all samples with no cross-shaped pattern had ca. $\alpha^{aniso} = 6$ dB/km. Therefore, this radial birefringence increased the apparent α^{aniso} by 2 dB/km. This radial birefringence was caused presumably by adhesion between the sample and the inner wall of the glass tube during volume contraction when polymerizing or cooling the sample.

For instance, the sample polymerized at 130 and 180 °C in Table III showed the birefringence cross-shaped pattern, and $\alpha^{aniso} = 6.4$ dB/km and $\alpha_1^{iso} = 7.2$ kB/km. This apparent α_1^{iso} is smaller than the theoretical limitation in eq 18 by ca. 2 dB/km. Since V_{V1}^{iso} is obtained by taking $^4/_3 H_V$ from V_{V1} as written in eq 6, this discrepancy would be caused by the overestimation of H_V due to the above birefringence.

Conclusion

PMMA glasses, in which the light-scattering loss was much smaller than any reported data and no large heterogeneities existed, was prepared for the first time. The lowest total scattering loss α_t was 13 dB/km which represents an inherent limiting loss of the PMMA glass in the atmosphere.

The origins of the large heterogeneities which have been invariably observed in any reported PMMA glasses were investigated by the angular dependence of the scattering intensity.

(1) If small molecules such as remaining monomers are not localized, the small molecules present in concentrations of several weight percentages doe not seriously affect the excess scattering.

(2) The excess V_V intensity is intrinsically independent of the molecular weight of the polymer in the range $M_w = 4 \times 10^4$–1.2×10^5.

(3) Stereoregularity in the ranges of $P_h/P_s = 0.69$–0.93 is not the main origin of the excess scattering, although mechanical properties such as T_g were slightly changed.

(4) The formation of cross-links as the result of the "gel effect" was not observed even in the sample with a large excess scattering.

(5) A variety of V_V intensities of the samples prepared by various conditions were reduced near to the value predicted by the thermally induced fluctuation theory by giving the samples a sufficient heat treatment above T_g. It is suggested that isotropic strain inhomogeneities caused during polymerization are the dominant origin of the excess V_V scattering.

Registry No. PMMA, 9011-14-7; MP, 554-12-1.

References and Notes

(1) Flory, P. J. *Principles of Polymer Chemistry*; Cornell University Press: New York, 1953.
(2) Fischer, E. W.; Dettenmaier, M. *J. Non-Cryst. Solids* **1978**, *31*, 181.
(3) Kargin, V. A. *J. Polym. Sci.* **1958**, *30*, 247.
(4) Yeh, G. S. Y. *J. Macromol. Sci.* **1972**, *B6*, 465.
(5) Pechhold, W.; Hauber, M. E. T.; Liska, E. *Kolloid-Z. Z. Polym.* **1970**, *241*, 955.
(6) Yeh, G. S. Y.; Geil, P. H. *J. Macromol. Sci.* **1967**, *B1*, 235.
(7) Kirste, R. G.; Kruse, W. A.; Schelten, J. *Macromol. Chem.* **1972**, *162*, 299.
(8) Ballard, D. G. H.; Wignall, G. D.; Schelten, J. *Eur. Polym. J.* **1973**, *9*, 965.
(9) Wendorff, J. H.; Fischer, E. W. *Kolloid-Z. Z. Polym.* **1973**, *251*, 884.
(10) Fischer, E. W.; Wendorff, J. H.; Dettenmaier, M.; Lieser, G.; Voigt-Martin, I. *J. Macromol. Sci. Phys.* **1976**, *B12*, 41.
(11) Tanabe, Y.; Muller, N.; Fischer, E. W. *Polym. J.* **1984**, *16*, 445.
(12) Patterson, G. D. *J. Macromol. Sci. Phys.* **1976**, *B12*, 75.
(13) Misra, A.; David, D. J.; Snelgrove, J. A.; Matis, G. *J. Appl. Polym. Sci.* **1986**, *31*, 2387.
(14) Yamashita, T.; Shichijyo, S.; Takemura, T.; Matsushige, K. *Jpn. J. Appl. Phys. Part 2* **1987**, *26*, L1797.
(15) Cielo, D.; Favis, B. D.; Maldague, X. *Polym. Eng. Sci.* **1987**, *27*, 1601.
(16) Patterson, G. D. *Annu. Rev. Mater. Sci.* **1983**, *13*, 219.
(17) Fujiki, M.; Kaino, T.; Oikawa, S. *Polym. J.* **1983**, *15*, 693.
(18) Dettenmaier, M.; Fischer, E. W. *Kolloid-Z. Z. Polym.* **1973**, *251*, 922.
(19) Judd, R. E.; Crist, B. *J. Polym. Sci., Polym. Lett. Ed.* **1980**, *18*, 717.
(20) Shichijyo, S.; Matsushige, K.; Takemura, T. *Mem. Fac. Eng. Kyushu Univ.* **1985**, *45*, 225.
(21) Ohtsuka, Y.; Koike, Y.; Awaji, H.; Tanio, N. *Kobunshi Ronbunshu* **1985**, *42*, 265.
(22) Claiborne, C.; Crist, B. *Colloid Polym. Sci.* **1979**, *257*, 457.
(23) Koike, Y.; Tanio, N.; Ohtsuka, Y. *Prepr. 2nd SPSJ International Polymer Conf. (Tokyo)* **1986**, 134.
(24) Kaino, T. *Appl. Phys. Lett.* **1986**, *48*, 757.
(25) Koike, Y.; Takezawa, Y.; Ohtsuka, Y. *Appl. Opt.* **1988**, *27*, 486.
(26) Pike, E. R.; Pomeroy, W. R. M.; Vaughan, J. M. *J. Chem. Phys.* **1975**, *62*, 3188.
(27) Kerker, M. The *Scattering of Light and Other Electromagnetic Radiation*; Academic Press: New York, 1972.
(28) Debye, P.; Anderson, H. R.; Brumberger, H. *J. Appl. Phys.* **1957**, *28*, 679.
(29) Einstein, A. *Ann. Phys.* **1910**, *33*, 1275.
(30) Vorenkamp, E. J.; Bosscher, F.; Challa, G. *Polymer* **1979**, *20*, 59.
(31) Suzuki, H.; Hiyoshi, T.; Inagaki, H. *J. Polym. Sci., Polym. Symp.* **1977**, *61*, 291.
(32) Kato, Y.; Nishioka, A. *Bull. Chem. Soc. Jpn.* **1964**, *37*, 1614.
(33) Bovey, F. A.; Tiers, G. V. D. *J. Polym. Sci.* **1960**, *44*, 173.
(34) Mitchell, R. S.; Guillet, J. E. *J. Polym. Sci., Polym. Phys. Ed.* **1974**, *12*, 713.
(35) Tanio, N.; Koike, Y.; Ohtsuka, Y. *Polym. J.* **1989**, in press.